

ac Josephson effect in finite-length nanowire junctions with Majorana modes

Pablo San-Jose¹, Elsa Prada², Ramón Aguado²

¹*Instituto de Estructura de la Materia (IEM-CSIC), Serrano 123, 28006 Madrid, Spain*

²*Instituto de Ciencia de Materiales de Madrid (ICMM-CSIC), Cantoblanco, 28049 Madrid, Spain*

(Dated: November 25, 2021)

It has been predicted that superconducting junctions made with topological nanowires hosting Majorana fermions exhibit an exotic Josephson effect which, owing to fermionic parity conservation, is 4π -periodic in the superconducting phase difference. Finding an experimental setup with these unconventional properties poses, however, a serious challenge: for finite-length junctions, the equilibrium supercurrents are always 2π -periodic as anticrossings of states with the same parity are possible. Landau-Zener transitions, induced by a dc bias voltage, are a conceivable route to revealing the 4π effect. However, inelastic processes are expected to induce parity-mixing quasiparticle poisoning and hence destroy the anomalous periodicity. We here demonstrate that this intuition may be wrong: the ac Josephson current retains its anomalous 4π -periodic components during long-lived transients in the topological phase. Remarkably, quasiparticle escape towards the contacts can induce a quantum Zeno effect which fixes the parity of the Majorana logical qubits and delays the decay of transients. Hence, transient spectral properties may be effectively used to detect Majorana states.

PACS numbers: 03.65.Vf 73.21.Hb 74.50.+r

Majorana fermions, a real solution of the Dirac equation discovered by Ettore Majorana in 1937, may appear in condensed matter as emergent low-energy excitations [1–4] with Non-Abelian statistics [5, 6]. Early examples of materials predicted to host such excitations include exotic superconductors with p-wave pairing [7, 8]. Recently, it has been predicted that Majorana quasiparticles should also appear in topological insulators [9] and semiconductors with strong spin-orbit coupling [10–13] which, in proximity to s-wave superconductors, may behave as topological superconductors (TS). Majorana bound states (MBS) in these TS can be understood as Bogoliubov-De Gennes quasiparticles (a superposition of an electron and a hole) appearing inside the superconducting gap, exactly at zero energy (for a review see Ref. 14). MBS come in pairs and are located at the edges of the nanowire or wherever the system interfaces with a non-topological phase. [15].

The TS phase transition is tunable, which has spurred a great deal of experimental activity towards detecting MBS in hybrid superconductor-semiconductor systems by, e.g., measuring the Josephson effect through a junction between two TS nanowires (for alternative schemes see Refs. 16–22). Kitaev predicted [23] that such Josephson effect has an anomalous 4π -periodicity in the superconducting phase difference $\phi \equiv \phi_1 - \phi_2$ between the two wires. This *fractional* Josephson effect $I_J \sim \sin(\frac{\phi}{2})$ may be interpreted as tunneling of half a Cooper pair through the zero-energy MBS inside the superconducting gap and is ubiquitous in superconducting junctions with MBS [12, 13, 23–28]. The 4π -periodicity can be understood in terms of fermion parity: if fermionic parity is *preserved*, the system *cannot* remain in the ground state as ϕ evolves from 0 to 2π adiabatically; the reason being that the ground state parity changes when $\phi \rightarrow \phi + 2\pi$. This gives rise to a protected crossing at $\phi = \pi$ [29] and hence to a perfect population inversion due to the or-

thogonality of the two Majorana states.

It has been argued [30] that finite length effects (neglected in all the previous works) render the Josephson effect 2π -periodic: any finite length of the TS region gives rise to hybridization of states of the same parity and a residual splitting, namely *anticrossings* at $\phi = \pi$. In an adiabatic situation, any such splitting (despite being exponentially small) will destroy population inversion, and hence the fractional effect in the equilibrium supercurrents. As it turns out, the splitting arises by the hybridization of the two MBS in the junction with two additional MBS that develop at the opposite end of each wire, which are linked to the (topologically trivial) external circuit.

The 4π -periodicity can be restored in two ways. On the one hand, one may employ a fully topological circuit [31]. In other words, by employing an S'NS' geometry (where S' is a TS and N is a normal, non-topological one), as opposed to an SS'NS'S junction (where S is a topologically trivial superconductor). Unfortunately, this is presently a difficult experimental challenge using semiconducting wires. Alternatively, the anomalous 4π Josephson effect may be recovered by biasing the junction and thereby sweeping ϕ fast enough through the anticrossing such that Landau-Zener (LZ) processes [32] induce non-adiabatic transitions between states of the same parity. By the same token, however, nonadiabatic transitions to the continuum of states above the gap will be unavoidable. Such processes are expected to once more spoil the fractional Josephson effect by parity mixing (quasiparticle poisoning) [33].

The above hindrances pose relevant questions. Is the Josephson effect a useful tool to detect MBS in TS nanowires? Do finite TS length and quasiparticle poisoning inevitably destroy the fractional periodicity? We here prove that the ac currents contain anomalously long-lived 4π -periodic transients in the TS phase. Thus, the

Josephson effect may still be exploited to provide unequivocal proof of the existence of MBS in finite-length TS. The nontrivial dynamics of the TS junction are summarized in a diagram of the ac current as a function of the Josephson frequency and the transmission of the normal part, with large regions of 4π -periodicity with a superimposed beating envelope owing to incomplete LZ transitions. These regions are tunable through both bias and gate voltages.

Interestingly, the duration of the long 4π -periodic transients may be increased by the well-known, though somewhat counter-intuitive, *quantum Zeno effect*, whereby a strong coupling to a decohering environment helps to confine the dynamics of a quantum system into a desired sector of the Hilbert space (quantum Zeno subspace [34]). Starting from a realistic Bogoliubov-De Gennes (BdG) model for the finite-length junction, we derive an effective description of the MBS dynamics that, by the escape of states above the TS gap, develops Zeno parity protection. This description allows us to solve the real-time ac Josephson problem and to characterize the transient and stationary regimes. A proper description of the evolution of the quasi-continuum of Andreev levels above the TS gap, which is well beyond the reach of simplified Kitaev models, is shown to be crucial to quantitatively assess its role in quasiparticle poisoning.

To the best of our knowledge, our work is the only theoretical study in the literature on the non-adiabatic ac Josephson dynamics of realistic TS nanowire junctions of finite length. We believe that our predictions should be realizable in state-of-the-art experiments with semi-conducting nanowires.

I. LOW-ENERGY DESCRIPTION OF FINITE LENGTH TOPOLOGICAL SUPERCONDUCTORS IN TERMS OF MAJORANA LOGICAL QUBITS.

Consider a semiconducting one-dimensional nanowire with small chemical potential $\mu_{S'}$, spin-orbit coupling α , and externally controllable Zeeman splitting \mathcal{B} (given by $\mathcal{B} = g\mu_B B/2$, where B is an in-plane magnetic field, μ_B is the Bohr magneton and g is the nanowire g-factor). When it is placed in contact with an s-wave superconductor of gap Δ_S , a superconducting pairing term $\Delta_{S'} < \Delta_S$ may be induced inside the nanowire by the proximity effect. The wire is then arranged into a Josephson device as illustrated in Fig. 1a, with a superconducting phase difference ϕ across the junction. The resulting hybrid system $SS'NS'S$ can be driven into a TS phase where two MBS are formed at the ends of each S' regions, denoted by $\gamma_{1,2}$ and $\gamma_{3,4}$. This is achieved by increasing the Zeeman splitting beyond a critical value $\mathcal{B} > \mathcal{B}_c \equiv \sqrt{\mu_{S'}^2 + \Delta_{S'}^2}$ [12, 13] (neglecting interaction corrections [35–37]). The low-energy Majorana sector appears for energies $\varepsilon < \Delta_{\text{eff}}$, where Δ_{eff} is the effective superconducting gap (see Fig. 2b).

Majorana bound states γ_i , when decoupled from each

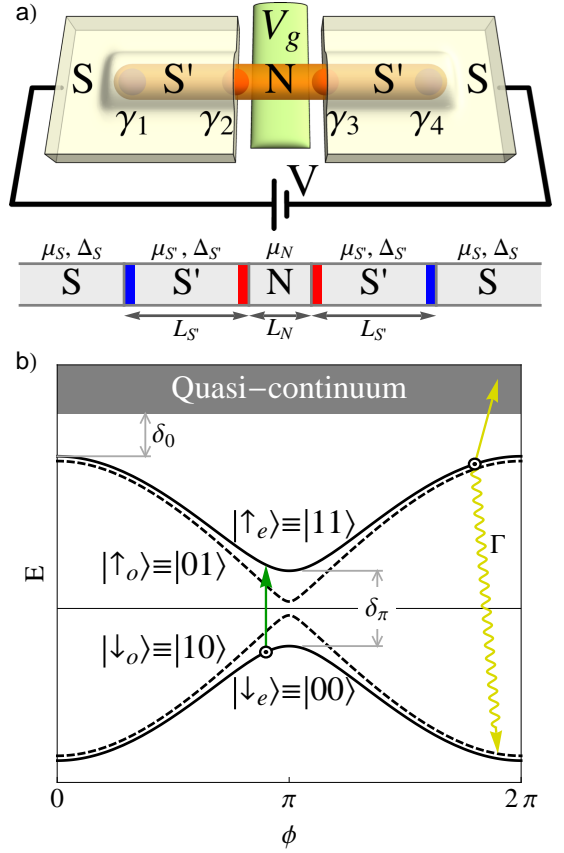


FIG. 1. (a) Schematics of the junction. A nanowire of length $L = L_{S'} + L_N + L_{S'}$ is in contact with two s-wave superconducting leads (with gap Δ_S), developing a proximity-induced superconducting gap $\Delta_{S'} < \Delta_S$. If the wire is longer than its spin-orbit length l_{so} and is subject to a strong enough longitudinal Zeeman field \mathcal{B} (larger than a critical \mathcal{B}_c), it will undergo a transition into a topological superconducting phase, which contains Majorana bound states at the interfaces between trivial non-trivial (SS' and NS') regions (a total of four Majorana states denoted by $\gamma_{1,2,3,4}$). The transparency of the junction can be controlled by a gate voltage V_g placed at the N region. (b) Energy of the four lowest many-body states of the junction in the topological phase, as a function of superconducting phase difference ϕ across N . They correspond to even and odd fillings of the two lowest Andreev bound states, see Fig. 2(b). Note the avoided crossing of size δ_π at $\phi = \pi$, that is due to the hybridization, for finite $L_{S'}$, of inner and outer Majorana modes (red and blue in (a), respectively). Driving ϕ with a bias voltage V , induces parity conserving transitions around $\phi = 2\pi(n + 1/2)$ (integer n), and parity breaking dissipative processes around $\phi = 2\pi n$, involving transitions into the quasi-continuum across the detachment gap δ_0 , which may be controlled through V_g .

other, are zero energy superpositions of a particle and a hole. By properly combining any pair of Majoranas $\gamma_{1,2}$, they may be fused into a Dirac fermion $c^\dagger = (\gamma_1 - i\gamma_2)/\sqrt{2}$, such that the operator $2c^\dagger c - 1 = 2i\gamma_1\gamma_2$ with eigenvalues -1 and 1 in states $|0\rangle$ and $|1\rangle = c^\dagger|0\rangle$ defines fermion parity. These parity states constitute an

Ising qubit, $\sigma_z = -2i\gamma_1\gamma_2$. One can represent a full spin with three MBS [38, 39] and thus a logical qubit may be constructed [40]:

$$\sigma_z = -2i\gamma_1\gamma_2; \sigma_y = -2i\gamma_3\gamma_1; \sigma_x = -2i\gamma_2\gamma_3. \quad (1)$$

A spatial overlap of two Majorana states hybridizes them into eigenstates of well defined and opposite parity, i.e. full (odd) and empty (even) states of the corresponding Dirac fermion. In a single TS wire of finite length $L_{S'}$, the decay distance of the two MBS pinned at the wire ends is the effective coherence length $\xi_{\text{eff}} = 2\hbar v_F / \pi \Delta_{\text{eff}}$. Their overlap will induce a splitting $\sim \pm \Delta_{\text{eff}} e^{-L_{S'}/\xi_{\text{eff}}}$. Similarly, two Majoranas at either sides of a Josephson junction with phase difference ϕ and transparency T will hybridize into even/odd fermion states with energies $\sim \pm \Delta_{\text{eff}} \sqrt{T} \cos \phi/2$, [24, 25, 33] which yields a parity inversion of the ground state as $\phi \rightarrow \phi + 2\pi$.

In the setup of Fig. 1, *four* MBS (two ‘inner’ $\gamma_{2,3}$ and two ‘outer’ $\gamma_{1,4}$) hybridize simultaneously both through the Josephson junction (region N) and the finite length S' wires. The resulting eigenstates are empty and filled states of two Dirac fermions $d_{1,2}^\dagger(\phi)$, constructed as two ϕ -dependent (orthogonal) superpositions of the two fermions $c_{in}^\dagger = (\gamma_2 + i\gamma_3)/\sqrt{2}$ and $c_{out}^\dagger = (\gamma_1 + i\gamma_4)/\sqrt{2}$, which are themselves obtained from the fusion of the inner and outer MBS, respectively. We denote eigenenergies by $E_{n_1 n_2}$ and eigenstates as $|n_1 n_2\rangle$, where $n_1, n_2 = 0, 1$ are the occupations of fermions d_1^\dagger and d_2^\dagger . Two of them have even *total parity*, $|\downarrow_e\rangle \equiv |00\rangle$, $|\uparrow_e\rangle \equiv |11\rangle = d_2^\dagger d_1^\dagger |00\rangle$, and the other two are odd, $|\downarrow_o\rangle \equiv |10\rangle = d_1^\dagger |00\rangle$, $|\uparrow_o\rangle \equiv |01\rangle = d_2^\dagger |00\rangle$. Thus, the Hilbert space of the four MBS is that of two *decoupled* replicas of the logical qubit in Eq. (1). The energy spectrum $E_{n_1 n_2}(\phi)$ exhibits anti-crossings at $\phi = \pi$ within same-parity sectors (Fig. 1b, solid and dashed curves correspond to even/odd states, respectively). The spectrum and, hence, the equilibrium supercurrents are 2π -periodic.

A 4π -periodic Josephson effect can, nevertheless, be recovered by inducing LZ transitions with a voltage bias, such as $|\downarrow_e\rangle \rightarrow |\uparrow_e\rangle$ (green arrow in Fig. 1b). To describe the response of a biased junction, however, an extension of the simplified two-spinor model above is required. Indeed, non-adiabatic driving may also induce inelastic transitions into delocalized states above the TS gap (yellow arrow in Fig. 1b). These latter transitions change the total parity of the system and induce an effective parity-mixing rate (yellow wiggly arrow) which couples even and odd sectors, namely quasiparticle poisoning. A proper description of such non-adiabatic dynamics involves a calculation of *all* the Andreev levels (both below and above Δ_{eff}) coupled to the continuum (above Δ_S) of the superconducting junction, which we develop in what follows.

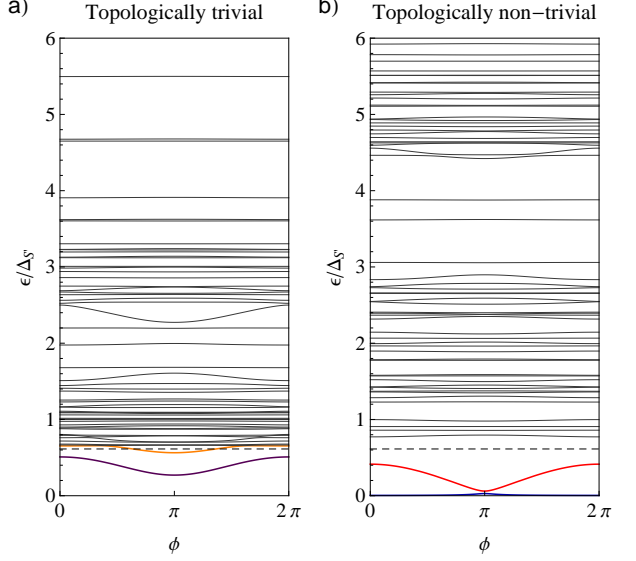


FIG. 2. Andreev bound states (ABS) for a Josephson SS'NS'S junction with normal conductance $G = 0.72G_0$ (where $G_0 = 2e^2/h$ is the conductance quantum), an induced gap $\Delta_{S'} = 218\mu\text{eV}$, and wire's total length of $4\mu\text{m}$ (where $l_{so} = 216\text{nm}$ for a InSb wire). In the topologically trivial phase (a), $\mathcal{B} = 0.36\text{meV} = 0.5\mathcal{B}_c$, whereas in the non-trivial phase (b), $\mathcal{B} = 1.1\text{meV} = 1.5\mathcal{B}_c$. The dashed line denotes the effective gap $\Delta_{\text{eff}} = 0.13\text{meV}$ in the wire, which separates localized ABS and those extended along the whole wire (quasi-continuum). In the topological case (b), Δ_{eff} is defined as the smallest of the two gaps $\Delta_1 \equiv |\mathcal{B} - \mathcal{B}_c|$ and $\Delta_2 \equiv \Delta_{S'} \sqrt{\frac{2(1+\tilde{\mu}) + \sqrt{1+2\tilde{\mu}+\tilde{\mathcal{B}}^2}}{\tilde{\mathcal{B}}^2 + 2(1+\tilde{\mu}) + \sqrt{1+2\tilde{\mu}+\tilde{\mathcal{B}}^2}}} + \mathcal{O}(\Delta_{S'}^2)$, with tilde quantities denoting energies in units of the spin-orbit energy, $E_{so} \equiv \hbar^2/m^*l_{so}^2$, with $l_{so} \equiv \hbar^2/m^*\alpha$ the spin-orbit length given in terms of the wire's effective mass m^* and spin-orbit coupling α .

II. FULL ANDREEV LEVEL SPECTRUM.

The full spectrum of single-particle eigenstates in the junction, including the $d_{1,2}^\dagger$ states, may be obtained by numerically diagonalizing the BdG equations for the geometry in Fig. 1a (see Appendix). We obtain $H_{\text{BdG}} = \frac{1}{2} \sum_n (d_n^\dagger d_n - d_n d_n^\dagger) \varepsilon_n$, with eigenenergies $\varepsilon_n(\phi)$ plotted in Fig. 2a,b for a representative junction, before and after the TS transition. The corresponding single particle excitations, called Andreev bound states (ABS), are defined as $|n(\phi)\rangle = d_n^\dagger(\phi)|\Omega(\phi)\rangle$, with $|\Omega(\phi)\rangle$ denoting the ground state. In the short junction limit, $L_N \ll \xi_{\text{eff}}$, only two ABS lie below the effective gap Δ_{eff} . Upon crossing into the TS phase, these two levels, initially localized around the N region in the non-topological phase (purple and orange curves in Fig. 2a), reconnect into the two $d_{1,2}^\dagger(\phi)$ Majorana branches. The lowest Majorana branch (blue curve in Fig. 2b, level d_1^\dagger) has a weak ϕ energy dependence, and is dominated by the outer MBS (c_{out}^\dagger fermion, $\varepsilon_1 \approx \Delta_{\text{eff}} e^{-L_{S'}/\xi_{S'}}$), whereas the one at higher

energy (red curve, d_2^\dagger) results mostly from the fusion of the inner MBS (c_{in}^\dagger fermion, $\varepsilon_2 \approx \Delta_{\text{eff}}\sqrt{T}\cos\phi/2$).

Due to the finite length $L_{S'} > \xi_{S'}$, a dense set (quasi-continuum) of ABS delocalized across the TS wire appear within a large energy window $\Delta_S > \varepsilon > \Delta_{\text{eff}}$ above the low-energy sector. This quasi-continuum (which approaches a continuum as $L_{S'} \rightarrow \infty$), separates the Majorana branches from the true continuum of the problem at $\varepsilon > \Delta_S$. Importantly, for finite transparency junctions, the Majorana levels detach from the quasi-continuum, as opposed to the topologically trivial case or a standard SNS junction [41] where the ABS touch the continuum at $\phi = 0, 2\pi$. We have verified that the detachment, denoted by δ_0 in Fig. 1b, increases as the transmission T of the normal region becomes smaller, $\delta_0/\Delta_{\text{eff}} \approx 1 - \sqrt{T}$, in agreement with simpler models [24, 25, 33]. Parity mixing in the low energy Majorana sector by quasiparticle escape into the quasi-continuum is, therefore, mediated by coherent transitions across the gap δ_0 , which profoundly affects the parity dynamics, as shown in what follows.

III. NON-ADIABATIC DYNAMICS.

We are now ready to analyze the non-adiabatic dynamics of the SS'NS'S junction, in search for signatures of the MBS. We study the Josephson current across the junction, or more generally its density matrix, when biased with a voltage V . The bias makes the phase difference ϕ time dependent, $\phi(t) = 2eVt/\hbar = \omega_J t$, where ω_J is the Josephson frequency. In the absence of quasiparticle poisoning (completely ignoring the levels above Δ_{eff}), the density matrix $\rho(t)$, written in the basis of the four instantaneous eigenstates $|n_1 n_2(\phi)\rangle$, would remain block diagonal in the even/odd subspaces, and its evolution would be completely coherent. Importantly, since the instantaneous eigenstates are ϕ (and hence time) dependent, the Hamiltonian \mathcal{H} dictating the Liouville von Neumann equation

$$\partial_t \rho(t) = -\frac{i}{\hbar} [\mathcal{H}(t), \rho(t)] \quad (2)$$

is not simply H_{BdG} projected into the Majorana sector: it also includes geometric connections $\mathcal{A}_{n'_1 n'_2, n_1 n_2} \equiv i\langle n'_1 n'_2 | \partial_\phi | n_1 n_2 \rangle$ between basis elements with the same parity, which are responsible for the LZ transitions within each sector, including the production of fermion pairs [11] from the ground state $|00\rangle$ (see Appendix).

Adding back the levels above Δ_{eff} opens up the possibility of quasiparticle exchange with the quasi-continuum. To account for such quasiparticle poisoning, one could pursue a brute-force approach by including an extended basis with all many-body states generated by filling the first N Andreev levels in the spectrum, Fig. 2. [42] This is impractical, however, since the size of the basis grows exponentially as 2^N . Moreover, it soon becomes clear that once a fermion fully escapes from

the Majorana sector, it has a vanishing probability of returning, given the large phase space available in the quasi-continuum. This allows one to adopt a more efficient strategy by introducing a Markovian fermion decay rate $\Gamma_0^{(m)}$ in each level $\varepsilon_{m \geq 3}$ that models the escape of quasiparticles from said level. In the fast decay limit $\Gamma_0^{(m)} \gg \omega_J$, this strategy allows one to trace out all the quasi-continuum, reducing the problem to a Markovian evolution of the *reduced* density matrix $\tilde{\rho}$ within the Majorana sector. Its master equation acquires an additional parity-mixing Lindblad term, see Appendix,

$$\partial_t \tilde{\rho} \approx -\frac{i}{\hbar} [\mathcal{H}, \tilde{\rho}] + \sum_{\alpha\beta} \Gamma_{\alpha\beta} \left(\mathcal{L}_\alpha \tilde{\rho} \mathcal{L}_\beta^\dagger - \frac{1}{2} \{ \mathcal{L}_\beta^\dagger \mathcal{L}_\alpha, \tilde{\rho} \} \right) \quad (3)$$

with four parity-mixing Lindblad operators,

$$\begin{aligned} \mathcal{L}_1 &= |\downarrow_e\rangle\langle\uparrow_o| + |\downarrow_o\rangle\langle\uparrow_e| \\ \mathcal{L}_2 &= |\downarrow_e\rangle\langle\downarrow_o| - |\uparrow_o\rangle\langle\uparrow_e| \\ \mathcal{L}_3 &= -|\uparrow_e\rangle\langle\uparrow_o| + |\downarrow_o\rangle\langle\downarrow_e| \\ \mathcal{L}_4 &= |\uparrow_e\rangle\langle\downarrow_o| + |\uparrow_o\rangle\langle\downarrow_e| \end{aligned} \quad (4)$$

and a 4×4 relaxation matrix

$$\Gamma_{\alpha\beta}(\phi) = 4\omega_J^2 \sum_m \frac{\nu_{m\alpha}^*(\phi) \nu_{m\beta}(\phi)}{\Gamma_0^{(m)}}. \quad (5)$$

The $\vec{\nu}_m(\phi)$, given explicitly in terms of single-particle connections in the Appendix, Eq. (12), are peaked at around $\phi = 2\pi n$, for integer n . They quantitatively account for parity mixing mediated by coherent excitation into dissipative level m , and contain detailed microscopic information about the quasi-continuum, making the resulting dynamics for the reduced density matrix highly non-trivial.

IV. AC JOSEPHSON EFFECT.

Since the levels $\varepsilon_{m \geq 3}$ above Δ_{eff} are almost ϕ independent, the Josephson current through the biased junction may be approximated in terms of the 4×4 reduced density matrix in the Majorana sector, namely the $\tilde{\rho}_{n_1 n_2, n'_1 n'_2} = \langle n_1 n_2 | \rho | n'_1 n'_2 \rangle$ governed by Eq. (3). Then

$$I(t) = \frac{4e}{\hbar} \sum_{n_1, n_2 = \{0,1\}} \tilde{\rho}_{n_1 n_2, n_1 n_2}(t) \partial_\phi E_{n_1 n_2}(\phi(t)), \quad (6)$$

where the many body energies E_{n_1, n_2} are the Majorana branches of Fig. 1b. Solving $\tilde{\rho}(t)$ with Eq. (3), we compute the Josephson current under bias V , assuming the junction is initially in its ground state $|\Omega(0)\rangle$ (at time $t = 0$). The goal is to identify smoking-gun features in $I(t)$, in the form of fractional frequency components, than may unambiguously determine the existence of MBS in the TS phase. It has been shown, however, that in the presence of finite dissipation (e.g. non-zero parity mixing as described above), the current becomes, in the long

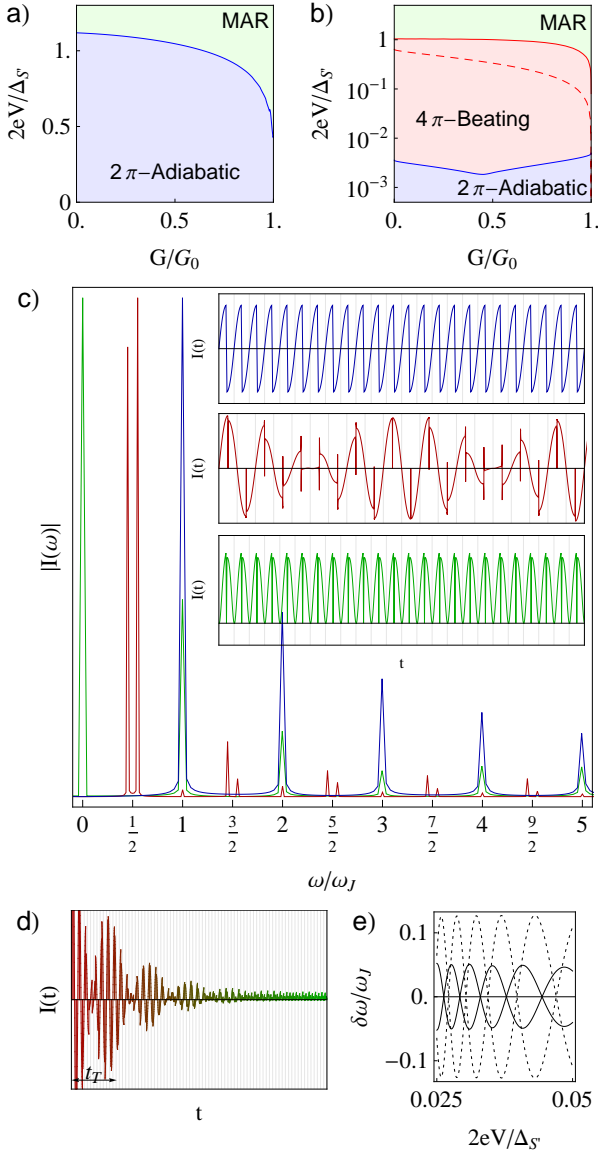


FIG. 3. Top: diagrams of the different dynamical regimes of the ac Josephson current as a function of junction bias V and dimensionless conductance G/G_0 , for (a) the topologically trivial and (b) non-trivial phases of a $8.7\mu\text{m}$ long InSb wire similar to that of Fig. 2. The different current behaviours (including 30 ABS from the quasi-continuum) are presented in (c), together with their distinct frequency transforms. These include the conventional adiabatic (blue) and multiple Andreev reflection (MAR) (green) regimes, both 2π -periodic. Note the appearance of a wide region of 4π -periodic ac Josephson effect (red) in the non-adiabatic TS phase, which is absent in the trivial case. In a finite length SS'NS'S setup, this fractional Josephson is revealed as a long-lived, transient regime that exhibits a superimposed beating pattern, evident as a split $\omega_J/2$ peak in the frequency spectrum. Panel (d) presents a typical dissipative decay from the 4π regime into the stationary MAR regime, which develops a dc current component (peak at $\omega = 0$). Panel (e) shows the spectral splitting $\pm\delta\omega$ as a function of the bias V of the anomalous peak at $\omega_J/2$ in the TS phase, both for the even (solid) and the odd sectors (dashed).

time limit, strictly 2π -periodic, as a consequence of Floquet theorem, and that as a result nothing remains in the stationary current to qualitatively distinguish the trivial from the TS phase [33, 43].

The two phases, however, exhibit crucial differences in their spectra that give rise to very different features in the transient regime, $I(t < t_T)$. The differences arise as a result of the sharp anticrossing at $\phi = \pi$, and the finite detachment in the TS phase between the *two* lower ABS and the quasi-continuum. In the trivial phase, in contrast, at least one of the two ABS merges into the quasi-continuum at $\phi = 0$ (modulo 2π , see orange curve in Fig. 2a). This spectral structure allows the even and odd Majorana subspaces in the TS phase to evolve almost coherently performing 4π -periodic population oscillations during a potentially long transient time $t_T \gg T_{2\pi}$, where $T_{2\pi} = 2\pi/\omega_J$ is the period of the Josephson driving. We now characterize the transient regime in detail.

The evolution of the TS junction depends strongly on the bias voltage. At bias $2eV < \delta_\pi$, the junction will remain in the initial ground state $|00\rangle$, resulting in an adiabatic 2π -periodic current (blue curve in Fig. 3c, inset), arising from $\partial_\phi E_{00}(\phi)$. Increasing $2eV$ above δ_π induces LZ transitions at $\phi = \pi$ from $|\downarrow_e\rangle = |00\rangle$ into $|\uparrow_e\rangle = |11\rangle$, which tend to produce a perfect population inversion as $2eV \gg \delta_\pi$. Then, if V remains smaller than a certain V_{MAR} (quantified in the next section), the population escape into the quasi-continuum as ϕ crosses 2π will be negligible, and the junction will subsequently re-invert into its ground state $|\downarrow_e\rangle$ at $\phi = 3\pi$. The repetition of this inversion process gives rise to a transient 4π -periodic Josephson current $I \sim \sin \phi/2$ (red curve in Fig. 3c, inset), with a superimposed beating envelope (due to imperfect LZ transitions for finite V at $\pi, 3\pi, 5\pi$, etc.). The parameter window required by this solution, $\delta_\pi \ll 2eV \ll 2eV_{\text{MAR}}$, is experimentally relevant, since δ_π and V_{MAR} may be independently controlled by the wire length $L_{S'}$ and e.g. the junction transparency, respectively.

In contrast, in the topologically trivial phase, only the lowest of the two Andreev levels in state $|11\rangle$ is detached from the quasi-continuum. Thus, the state will immediately decay into $|10\rangle$ upon crossing $\phi = 2\pi$. As a consequence, the 4π -periodic current cannot develop. The anomalous 4π -periodic component in the transient regime, therefore, is an unequivocal signature of the existence of MBS in the junction.

At high voltages approaching $V \sim V_{\text{MAR}}$, the transition into the continuum becomes significant in each period $T_{2\pi}$, for both phases. For such voltages, the transient time t_T becomes comparable to $T_{2\pi}$, and close to two fermions escape into the contacts per cycle. This process yields a finite dc current component (green curve in Fig. 3c, inset), which is the analogue of the multiple Andreev reflection (MAR) mechanism of conventional Josephson junctions. It should be noted that the current for *any* finite bias V eventually develops, in the stationary regime, a finite dc current component, that has the same origin as

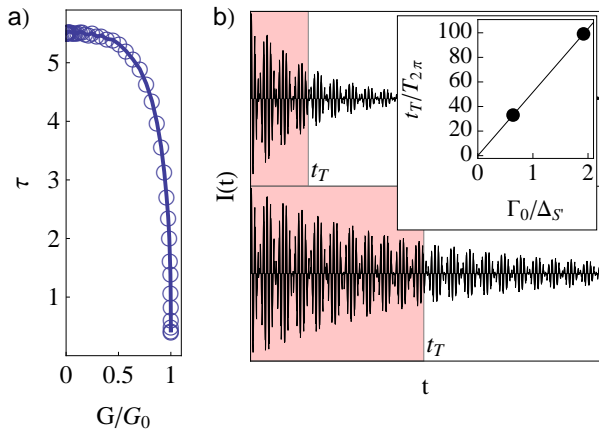


FIG. 4. Transient time scales as $t_T \equiv \frac{\hbar^2 \Gamma_0}{(2eV)^2} \tau$, with dimensionless function $\tau(G/G_0)$ plotted in (a). Due to the quantum Zeno effect, the dissipative decay of the transient 4π -beating regime (red shaded region, b) becomes slower as the relaxation rates in the quasi-continuum $\Gamma_0^{(m)}$ (assumed equal to Γ_0 for all m in the plot) increase. The two main panels in (b) show the ac Josephson current vs. time and correspond to $2eV = 0.03\Delta_S$, and two values of Γ_0 highlighted in the inset, which shows the transient time $t_T \propto \Gamma_0$.

MAR, i.e., the promotion of Cooper pairs into the quasi-continuum by iterated scattering processes in the biased junction (see Fig. 3d).

A parametric diagram of the MAR (green), the 2π -adiabatic (blue), and the 4π -beating (red) regimes possible are presented in Fig. 3a,b. The boundaries between regimes are crossovers, defined by $V = V_{\text{MAR}}$ and $2eV = \delta_\pi$. The different regimes may be clearly distinguished using a finite time spectral analysis of the current, shown in Fig. 3c. The adiabatic regime exhibits frequency components at $\omega = n\omega_J$, for integer $n > 0$, while the MAR regime develops an additional $\omega = 0$ peak. The unique 4π -periodic transient regime in the TS phase, on the other hand, exhibits a distinct half-integer spectrum $\omega = (n + \frac{1}{2})\omega_J$, together with a peak splitting due to the accompanying beating envelope. The splitting, of magnitude $\pm\delta\omega$, is plotted in Fig. 3e as a function of the applied bias, which reveals oscillations due to the interference of successive LZ processes at odd multiples of $\phi = \pi$.

V. TRANSIENT TIMES, ZENO EFFECT AND PARITY FIXING.

The duration of the transient regime t_T in the TS phase is dictated by the characteristic decay time of the transient Josephson current $I(t) \sim e^{-t/t_T}$. Since this exponential decay is produced by the decay matrix Γ in Eq. (5), t_T scales with bias V and characteristic relaxation

rate Γ_0 as

$$t_T \equiv \frac{\hbar^2 \Gamma_0}{(2eV)^2} \tau \quad (7)$$

for some dimensionless τ that depends solely on the junction's normal conductance, $\tau(G/G_0)$ (assuming an m -independent $\Gamma_0^{(m)} = \Gamma_0$). Function τ is numerically computed in Fig. 4a. It is maximum in the tunneling regime and it decays to zero as transparency goes to one. This means that t_T decreases when the detachment $\delta_0 \rightarrow 0$, since then, the escape probability into the quasi-continuum in each cycle p goes to one. Such result is in accordance with the naive estimate of p in terms of the LZ probability $p = e^{-\pi\delta_0/eV}$. For non-perfect transparency, however, such LZ analysis would predict a characteristic escape voltage $2eV_{\text{MAR}} = \delta_0$ (red dashed line in Fig. 3b), which can be quite smaller than the correct result (solid red line), determined from the condition $t_T = T_{2\pi}$ in Eq. (7):

$$2eV_{\text{MAR}} = \hbar\Gamma_0\tau/2\pi.$$

In view of Eq. (7), one can see that, while a sufficiently slow driving V will suppress quasiparticle poisoning and will thus increase the duration of the transient regime, a complementary, and potentially preferable route is to engineer the environment's Γ_0 in order to increase the lifetime of the Majorana qubits without slowing operation. Indeed, by increasing the escape rates $\Gamma_0^{(m)}$ in Eq. (5), parity mixing will be suppressed, increasing t_T . This is known as the *quantum Zeno effect*, whereby a quantum system coupled to a bath may develop longer coherence times when increasing the speed at which information is lost into the bath. In a very fast environment (large $\Gamma_0^{(m)}$), the transitions into the quasi-continuum at $\phi = 2\pi n$ will be suppressed by this same Zeno mechanism. This is demonstrated in the simulation of Fig. 4b, which shows how the transient time t_T is tripled as a result of increasing the $\Gamma_0^{(m)}$ proportionally.

VI. DISCUSSION AND EXPERIMENTAL DETECTION.

Parity protection by the Zeno effect should prove useful for prolonging the 4π -periodic transient regime when the main source of quasiparticle poisoning is through the quasi-continuum. Other sources of poisoning not discussed here include non-equilibrium quasiparticles from the rest of the circuit, a contrition that can, however, be greatly reduced by including quasiparticle traps, such as nearby metal contacts [44]. In the case of quasicontinuum poisoning, a rough estimate relating the quasiparticle escape velocity to the Fermi velocity yields $\Gamma_0 \approx \Delta_{\text{eff}}$, which suggests that increasing Δ_{eff} will improve Zeno-type parity protection of driven Majorana qubits. Using realistic parameters for InSb nanowires, we estimate that

typical transient times reach into the μs range at μV bias voltages.

Owing to these long transient times, the spectrum of microwave radiation from TS junctions should show clear features of the fractional frequencies (Fig. 3c). Such measurement can be performed with an on-chip detector, which greatly minimizes the impedance-matching problems in classical detection schemes. This on-chip detection can be achieved by using, for example, the photon assisted tunneling current of quasiparticles across a superconductor-insulator-superconductor junction capacitively coupled to the TS one. Importantly, it has been *already* demonstrated [45] that such technique allows a direct detection of fractional Josephson frequencies [46]. This is possible if $T_1 \gg t_T$, where T_1 is the relaxation time corresponding to the transition $|\uparrow_e\rangle = |11\rangle \rightarrow |\downarrow_e\rangle = |00\rangle$ that brings the system back to the ground state. Such parity-conserving transitions, that at low enough temperatures are due to quantum fluctuations of the phase, can be attributed to photon emission to the electromagnetic environment and, to a lesser amount, to phonon emission. Proper engineering of the circuit containing the topological wire can, in principle, greatly reduce both emission processes. For example, photon emission can be inhibited by reducing the ohmic component of the impedance seen by the Majorana qubit [47], such that relaxation times of the order of $1\mu\text{s}$ can be achieved in realistic circuits (Appendix).

ACKNOWLEDGMENTS

Acknowledgments. We are grateful to Y. V. Nazarov, S. Frolov, L. Kowenhoven and S. Kohler for fruitful discussions. We acknowledge the support of the CSIC JAE-Doc program and the Spanish Ministry of Science and Innovation through grants FIS2008-00124/FIS (P.S.-J), FIS2009-08744 (E.P. and R.A.).

VII. APPENDIX.

The computation of the Andreev levels in an SS'NS'S junction is performed within the Nambu formulation of the junction Hamiltonian

$$H = \frac{1}{2} \int dx [\psi_\sigma^+(x), \psi_\sigma(x)] \quad (8)$$

$$\times \begin{bmatrix} H_{\sigma\sigma'}^{(0)}(x) & \Delta_{\sigma\sigma'}(x) \\ -\Delta_{\sigma\sigma'}^*(x) & -H_{\sigma\sigma'}^{(0)*}(x) \end{bmatrix} \begin{bmatrix} \psi_{\sigma'}(x) \\ \psi_{\sigma'}^+(x) \end{bmatrix}$$

where matrix $H^{(0)}(x)$ models the one-dimensional semi-conducting wire plus left and right leads, without superconducting pairing. It includes a constant transverse spin-orbit coupling α , a Zeeman field along the wire $\mathcal{B} = g\mu_B B/2$ (where B is an external magnetic field, μ_B is the Bohr magneton and g is the nanowire g-factor), and a position-dependent band shift $\mu(x)$ that accounts

for a larger electronic density in the leads than in the wire [12, 13],

$$H_{\sigma\sigma'}^{(0)}(x) = \frac{-\partial_x^2}{2m^*} + i\alpha\sigma_y\partial_x + \mathcal{B}\sigma_x - \mu(x).$$

We approximate $\mu(x)$ by a piecewise constant function, $\mu_{S'}$ in the wire, μ_N in the central normal region (controllable via a gate voltage V_g) and μ_S in the leads, see Fig. 1. The superconducting pairing also varies with x ,

$$\Delta_{\sigma\sigma'}(x) = -i\Delta(x)\sigma_y.$$

$\Delta(x)$ is assumed weaker in the superconducting part of the wire than in the leads $|\Delta_{S'}| < |\Delta_S|$, and zero in the central N region. We also denote the phase difference across the N region by ϕ , so that $\arg[\Delta(\pm|x|)] = \pm\phi/2$.

To compute the Andreev spectrum as a function of ϕ one may discretize the integral in Eq. (8), which approximates the continuum problem by a Nambu tight-binding chain. Exact diagonalization of the corresponding H matrix yields $H = \frac{1}{2} \sum_n (d_n^+ d_n - d_n d_n^+) \varepsilon_n$, where the single particle spectrum $\varepsilon_n(\phi)$ are the energies of the Andreev states $|n(\phi)\rangle = d_n^+(\phi)|\Omega(\phi)\rangle$ discussed in the main text, and $|\Omega(\phi)\rangle$ is the ground state. Alternatively, one may employ a wavematching method on the continuum model, and find the energies that yield normalizable solutions in the absence of incoming modes in the leads. We have checked that both methods yield the same results for a sufficiently fine tight-binding discretization, and exhibit band reconnection and Majorana branches if $\mathcal{B} > \sqrt{\Delta_{S'}^2 + \mu_{S'}^2}$, see Fig. 2b.

As a result of a bias V across the junction, the phase ϕ becomes time dependent, $\phi(t) = 2eVt/\hbar = \omega_J t$, and the system is driven out of equilibrium. For a given phase ϕ , one may build a set of many body instantaneous eigenstates $\{|\varphi_{\vec{n}}(\phi)\rangle = d^{+n_N} \dots d^{+n_1}|0\rangle\}$, where $n_m = 0, 1$ is the occupation of the m -th Andreev level and $H(\phi)|\varphi_{\vec{n}}(\phi)\rangle = E_{\vec{n}}(\phi)|\varphi_{\vec{n}}(\phi)\rangle$. The many body instantaneous energy is $E_{\vec{n}}(\phi) = \sum_m \varepsilon_m(\phi)(n_m - 1/2)$.

The time evolution of the system's full density matrix $\hat{\rho}(t)$ (note that this is different from the *reduced* density matrix in the main text) may be expressed in the $\{|\varphi_{\vec{n}}(t)\rangle\}$ basis, $\rho_{\vec{n}\vec{n}'}(t) \equiv \langle\varphi_{\vec{n}}(t)|\hat{\rho}(t)|\varphi_{\vec{n}'}(t)\rangle$, and is governed by the equation of motion,

$$\partial_t \rho(t) = -\frac{i}{\hbar} [\mathcal{H}(t), \rho(t)],$$

The effective Hamiltonian $\mathcal{H}(t)$ includes the connection between instantaneous eigenstates, $\mathcal{A}_{\vec{n}\vec{n}'}(\phi) \equiv i\langle\varphi_{\vec{n}'}(\phi)|\partial_\phi\varphi_{\vec{n}}(\phi)\rangle$,

$$\mathcal{H}_{\vec{n}\vec{n}'}(t) = \delta_{\vec{n},\vec{n}'} E_{\vec{n}}(\phi(t)) - \hbar [\partial_t \phi(t)] \mathcal{A}_{\vec{n}\vec{n}'}(\phi(t)).$$

The many body connection $\mathcal{A}_{\vec{n}\vec{n}'}$ may be related to the single particle connection $A_{nm} \equiv i\langle n|\partial_\phi|m\rangle = i\langle\Omega|d_n(\partial_\phi d_m^+)|\Omega\rangle$ [48] and the anomalous connection

$$\bar{A}_{nm} \equiv i\langle\Omega|(\partial_\phi d_m^+)d_n^+|\Omega\rangle \text{ by}$$

$$i\langle\varphi_{\bar{n}}|\partial_\phi|\varphi_{\bar{n}}\rangle = \sum_m A_{n_m n_m} \quad (9)$$

$$i\langle\varphi_{\bar{n}}|\partial_\phi d_i^+ d_j|\varphi_{\bar{n}}\rangle = -i\langle\varphi_{\bar{n}}|\partial_\phi d_i d_j^+|\varphi_{\bar{n}}\rangle^* = A_{ji} \quad (10)$$

$$i\langle\varphi_{\bar{n}}|\partial_\phi d_i^+ d_j^+|\varphi_{\bar{n}}\rangle = -i\langle\varphi_{\bar{n}}|\partial_\phi d_i d_j|\varphi_{\bar{n}}\rangle^* = \bar{A}_{ji} \quad (11)$$

for any state $|\varphi_{\bar{n}}\rangle$. All other connections are zero, which implies that the system evolution preserves fermion parity (i.e. if the initial number of excitations is definitely even or odd, it will remain that way, even though the total number may change due to the anomalous connection \bar{A} .)

Driving may impart the excitations with energy, which may coherently promote them into the quasi-continuum above Δ_{eff} . At that point, the excitation escapes (with a certain rate) towards the contacts, irreversibly to all practical effects. This single-fermion escape process changes parity. To model such two-step quasiparticle *poisoning* process without having to track the dynamics of the (exponentially) large number of many body states, one may substitute the single-particle quasi-continuum (h , or ‘high’) levels $|m\rangle_h$ by dissipative levels (with zero mutual connection) that decay directly into a fermion reservoir at a rate $\Gamma_0^{(m)}$, while the ‘low’ levels (l , below the gap) remain non-dissipative. If we assume a Markovian approximation for the decay of h into the fermionic bath, the master equation takes on a Lindblad form

$$\partial_t \rho = -\frac{i}{\hbar} [\mathcal{H}, \rho] + \sum_m \Gamma_0^{(m)} \left(L_m \rho L_m^\dagger - \frac{1}{2} \{L_m^\dagger L_m, \rho\} \right)$$

If we further constrain our dynamical space to states with a total of 1 or 0 fermions in the h sector, $\{|\varphi_{\bar{n}l;1_m}\rangle, |\varphi_{\bar{n}l;0}\rangle\}$ (fast decay limit), the Lindblad operators L_m will simply project any state with a fermion in the m -th dissipative level ($m \in h$), into another without it $L_m = \sum_{\bar{n}l} |\varphi_{\bar{n}l;0}\rangle\langle\varphi_{\bar{n}l;1_m}|$.

For large enough $\Gamma_0^{(m)} \sim \mathcal{O}(\eta^{-1})$ (η being a small perturbative parameter), the irreversible decay will suppress the density matrix in the quasi-continuum, $\rho_{ll} \sim \mathcal{O}(1)$, $\rho_{lh}, \rho_{hl} \sim \mathcal{O}(\eta)$, $\rho_{hh} \sim \mathcal{O}(\eta^2)$. One may then perturbatively solve the detailed balance conditions for the h

sector, which eventually leads to a Lindblad-type master equation for the reduced density matrix ρ_{ll} ,

$$\begin{aligned} \partial_t \rho_{ll} = & -\frac{i}{\hbar} [\mathcal{H}_{ll}, \rho_{ll}] \\ & + \sum_{\alpha\beta} \Gamma_{\alpha\beta} \left(\mathcal{L}_\alpha \rho_{ll} \mathcal{L}_\beta^\dagger - \frac{1}{2} \{ \mathcal{L}_\beta^\dagger \mathcal{L}_\alpha, \rho_{ll} \} \right) + \mathcal{O}(\eta) \end{aligned}$$

Considering the l sector as spanned by two Andreev levels, of energies $\varepsilon_{1,2}$, the corresponding many body basis $|\varphi_{n_1, n_2; 0}\rangle \equiv |n_1 n_2\rangle$ is $\{|\downarrow_e\rangle, |\uparrow_e\rangle, |\downarrow_o\rangle, |\uparrow_o\rangle\} \equiv \{|00\rangle, |11\rangle, |10\rangle, |01\rangle\}$, where e and o stand for even and odd fermion parity. Then, the Lindblad equation above reduces to Eq. (3) in the main text, where we denote ρ_{ll} simply by $\tilde{\rho}$. The effective Lindblad operators, given in Eq. (4), represent dissipative quasiparticle poisoning and couple even and odd sectors, The relaxation matrix reads,

$$\Gamma_{\alpha\beta} = 4\omega_J^2 \sum_m \frac{\nu_{m\alpha}^* \nu_{m\beta}}{\Gamma_0^{(m)}}$$

in terms of the single-particle connections between the l states and the h states,

$$\vec{\nu}_n = \{A_{2,n}, A_{1,n}, \bar{A}_{1,n}, \bar{A}_{2,n}\} \quad (12)$$

We finally calculate the efficiency of a different dissipative mechanism, namely the inelastic relaxation process by spontaneous photon emission into the electromagnetic environment, which is often a concern in electronic systems. To lowest order, the relaxation rate reads:

$$\begin{aligned} T_1^{-1} = & \frac{2\hbar}{\Delta E_e} \frac{1}{4e^2} |\langle\uparrow_e|\hat{I}|\downarrow_e\rangle|^2 \frac{\text{Re}[Z(\Delta E_e/\hbar)]}{R_K} \\ = & \frac{8\Delta E_e}{\hbar} |\langle\uparrow_e|\partial_\phi|\downarrow_e\rangle|^2 \frac{\text{Re}[Z(\Delta E_e/\hbar)]}{R_K}, \end{aligned} \quad (13)$$

where $\hat{I} = (4e/\hbar)\partial_\phi \mathcal{H}$, $\Delta E_e \equiv E_{\uparrow_e} - E_{\downarrow_e}$ and $R_K = \hbar/e^2 \approx 25.81 k\Omega$ is the resistance quantum. This rate is ϕ -dependent. Substituting the value of the connection between the even Majorana branches and their energy difference for the wire considered in Fig. 3, and averaging over the phase, we obtain relaxation times of the order of $1\mu\text{s}$ for impedances of $\text{Re}[Z(\Delta E_e/\hbar)] = 1\Omega$.

-
- [1] F. Wilczek, Nat. Phys. **5**, 614 (2009).
 - [2] M. Franz, Physics **3**, 24 (2010).
 - [3] T. L. Hughes, Physics **4**, 67 (2011).
 - [4] R. F. Service, Science **332**, 193 (2011).
 - [5] D. A. Ivanov, Phys. Rev. Lett. **86**, 268 (2001).
 - [6] A. Stern, Nature **464**, 187 (2010).
 - [7] G. Volovik, JETP Lett. **70**, 609 (1999).
 - [8] N. Read and D. Green, Phys. Rev. B **61**, 10267 (2000).
 - [9] L. Fu and C. L. Kane, Phys. Rev. Lett. **100**, 096407 (2008).
 - [10] J. D. Sau, R. M. Lutchyn, S. Tewari, and S. Das Sarma,

- Phys. Rev. Lett. **104**, 040502 (2010).
- [11] J. Alicea, Phys. Rev. B **81**, 125318 (2010).
- [12] R. M. Lutchyn, J. D. Sau, and S. Das Sarma, Phys. Rev. Lett. **105**, 077001 (2010).
- [13] Y. Oreg, G. Refael, and F. von Oppen, Phys. Rev. Lett. **105**, 177002 (2010).
- [14] C. W. J. Beenakker, arXiv:1112.1950v1 (2011).
- [15] J. Alicea, Y. Oreg, G. Refael, F. von Oppen, and M. P. A. Fisher, Nat. Phys. **7**, 412 (2011), using this property, MBS may be created and fused by applying locally tunable gates, which would allow braiding of Ma-

majorana fermions in nanowire networks.

- [16] C. J. Bolech and E. Demler, Phys. Rev. Lett. **98**, 237002 (2007).
- [17] J. Nilsson, A. R. Akhmerov, and C. W. J. Beenakker, Phys. Rev. Lett. **101**, 120403 (2008).
- [18] K. T. Law, P. A. Lee, and T. K. Ng, Phys. Rev. Lett. **103**, 237001 (2009).
- [19] K. Flensberg, Phys. Rev. B **82**, 180516 (2010).
- [20] L. Fu, Phys. Rev. Lett. **104**, 056402 (2010).
- [21] M. Wimmer, A. R. Akhmerov, J. P. Dahlhaus, and C. W. J. Beenakker, New Journal of Physics **13**, 053016 (2011).
- [22] A. Zazunov, A. L. Yeyati, and R. Egger, Phys. Rev. B **84**, 165440 (2011).
- [23] A. Y. Kitaev, Phys. Usp. **44**, 131 (2001).
- [24] H. Kwon, K. Sengupta, and V. Yakovenko, Eur. Phys. J. B **37**, 349 (2003).
- [25] L. Fu and C. L. Kane, Phys. Rev. B **79**, 161408 (2009).
- [26] P. A. Iosevich and M. V. Feigel'man, Phys. Rev. Lett. **106**, 077003 (2011).
- [27] K. T. Law and P. A. Lee, Phys. Rev. B **84**, 081304 (2011).
- [28] L. Jiang, D. Pekker, J. Alicea, G. Refael, Y. Oreg, and F. von Oppen, arXiv:1107.4102v1 (2011).
- [29] For the sake of the argument, we use a fixed value $\phi = \pi$ for the zero-energy crossing although its position is not universal, see, e. g. [12].
- [30] D. I. Pikulin and Y. V. Nazarov, JETP Lett. **94**, 752 (2011).
- [31] B. van Heck, F. Hassler, A. R. Akhmerov, and C. W. J. Beenakker, Phys. Rev. B **84**, 180502 (2011).
- [32] C. Wittig, J. Phys. Chem. B **109**, 8428 (2005).
- [33] D. M. Badiane, M. Houzet, and J. S. Meyer, Phys. Rev. Lett. **107**, 177002 (2011), this recent study considers the stationary ac Josephson current in junctions of helical edge states in two-dimensional topological insulators ($L_{S'} \rightarrow \infty$).
- [34] P. Facchi and S. Pascazio, Phys. Rev. Lett. **89**, 080401 (2002).
- [35] S. Gangadharaiah, B. Braunecker, P. Simon, and D. Loss, Phys. Rev. Lett. **107**, 036801 (2011).
- [36] E. Sela, A. Altland, and A. Rosch, Phys. Rev. B **84**, 085114 (2011).
- [37] E. M. Stoudenmire, J. Alicea, O. A. Starykh, and M. P. Fisher, Phys. Rev. B **84**, 014503 (2011).
- [38] A. M. Tsvelik, Phys. Rev. Lett. **69**, 2142 (1992).
- [39] A. Shnirman and Y. Makhlin, Phys. Rev. Lett. **91**, 207204 (2003).
- [40] C. Nayak, S. Simon, A. Stern, M. Freedman, and S. Das Sarma, Rev. Mod. Phys. **80**, 1083 (2008).
- [41] D. Averin and A. Bardas, Phys. Rev. Lett. **75**, 1831 (1995).
- [42] Note that although in some particular cases it is possible to describe the dynamics of the superconducting system within a single particle picture, while at the same time avoiding the double counting problem [49], this requires a block diagonal connection [50], a condition that is not generally satisfied, as in our case with non-zero Zeeman and spin-orbit couplings.
- [43] Yuli Nazarov, private communication and talk at <http://inac.cea.fr/Pisp/julia.meyer/workshop2011.html>.
- [44] M. Zgirski, L. Bretheau, Q. Le Masne, H. Pothier, D. Esteve, and C. Urbina, Phys. Rev. Lett. **106**, 257003 (2011).
- [45] P.-M. Billangeon, F. Pierre, H. Bouchiat, and R. Deblock, Phys. Rev. Lett. **98**, 216802 (2007).
- [46] Certain hybrid systems with strong Coulomb interactions, such as a quantum dot in the Kondo regime (see Ref. 51) or a superconducting single electron transistor, see P. Joyez, Ph.D. thesis, Paris 6 University (1995), may exhibit quasicontinuum detachment and a 4π Josephson effect, unrelated to the Majorana physics described here.
- [47] R. Aguado and L. P. Kouwenhoven, Phys. Rev. Lett. **84**, 1986 (2000).
- [48] The ground state connection may be gauged away without loss of generality.
- [49] N. M. Chtchelkatchev and Y. V. Nazarov, Phys. Rev. Lett. **90**, 226806 (2003).
- [50] J. Michelsen, V. S. Shumeiko, and G. Wendin, Phys. Rev. B **77**, 184506 (2008).
- [51] A. L. Yeyati, A. Martín-Rodero, and E. Vecino, Phys. Rev. Lett. **91**, 266802 (2003).